Nuclear Engineering and Technology 48 (2016) 925–931

Available online at ScienceDirect

Nuclear Engineering and Technology

journal homepage: www.elsevier.com/locate/net

Original Article

Analytical Modeling of Natural Convection in a Tall Rectangular Enclosure with Multiple Disconnected Partitions

Youngmin Bae[*], *Seong Hoon Kim*, *Jae-Kwang Seo*, *and Young In Kim*

Korea Atomic Energy Research Institute, 989-111 Daedeok-daero, Yuseong-gu, Daejeon, 34057, Republic of Korea

ARTICLE INFO

Article history:
Received 31 August 2015
Received in revised form
6 January 2016
Accepted 23 February 2016
Available online 29 March 2016

Keywords:
Buoyancy-Driven Flow
Natural Convection
Partitioned Enclosure

ABSTRACT

In this study, laminar natural circulation and heat transfer in a tall rectangular enclosure with disconnected vertical partitions inside were investigated. Analytical expressions were developed to predict the circulation flow rate and the average Nusselt number in a partially partitioned enclosure with isothermal side walls at different temperatures and insulated top and bottom walls. The proposed formulas are then validated against numerical results for modified Rayleigh numbers of up to 10^6. The impacts of the governing parameters are also examined along with a discussion of the heat transfer regimes.

1. Introduction

Enclosures divided by multiple vertical partitions are used in a wide variety of engineering applications such as mechanical, chemical, civil, and nuclear industries. Specifically, heat transfer through a partitioned enclosure has been of prime importance in the design of thermal insulators for nuclear reactors, buildings, cryogenic storage, etc.

The role of vertical partitions in suppressing the natural convection in enclosures heated from the sides has been extensively studied in the literature. Anderson and Bejan [1] conducted an experimental and theoretical study of natural convection in single and double partitioned enclosures, and reported that the heat transfer can be reduced by inserting vertical partitions. Nishimura et al. [2] investigated, both experimentally and numerically, laminar natural convection in rectangular enclosures with equally spaced vertical partitions inside. They showed that the heat transfer across the partitioned enclosure is inversely proportional to the number of fluid layers. A similar observation was made by Turkoglu and Yücel [3] for conducting partitions and side walls. Recently, Sambou et al. [4] presented a correlation to evaluate the average Nusselt number for partitioned enclosures with conducting side walls. There also have been several studies dealing with the effects of Rayleigh number, partition thickness and position, aspect ratio, and conductivity ratio of solid partition to fluid [5–8].

* *Corresponding author.*
E-mail address: ybae@kaeri.re.kr (Y. Bae).
http://dx.doi.org/10.1016/j.net.2016.02.021

Natural convection in enclosures with disconnected partitions inside has received little attention, although it is thought of as another major concern in practice. Costa et al. [9] conducted a numerical study on laminar free convection in enclosures with partial horizontal partitions. For enclosures with disconnected vertical partitions, Kim et al. [10] numerically investigated the thermal performance of the so-called wet thermal insulator installed in a system-integrated modular advanced reactor (SMART). When vertical partitions are disposed of inside the enclosure with gaps at the top and bottom ends to compensate for thermal expansion/contraction (see Fig. 1), buoyancy-driven flow circulates throughout the enclosure, i.e., fluid rises up in the hot-side layers, passing through the gap at the top, moving downward in the vertical channels near the cold side, and returning to the hot-side layers via the gap at the bottom. Compared to the case of connected partitions, in which natural circulation is confined within each fluid layer isolated by partitions, this often causes an undesirable increase in the circulation flow rate and heat transfer within the enclosure, significantly deteriorating the thermal insulation performance, as reported by Kim et al. [10]. Hence, if enclosures are used for thermal insulation purposes, it is desirable to remove the gaps by, for example, welding the partitioning plates to the top/bottom walls. However, owing to the limitations of the welding process associated with very thin partitioning plates and thermal expansion/contraction of materials in the case of integral-type nuclear reactors, it is often difficult in practice to eliminate the gaps and to ensure the perfect connection between them. Thus, in order to provide the proper requirements and/or recommendations for the design and manufacture of thermal insulator involving the selection of materials, we need to know in advance how the heat transfer performance is affected by the gaps, and to explore its functional dependence on the main governing parameters.

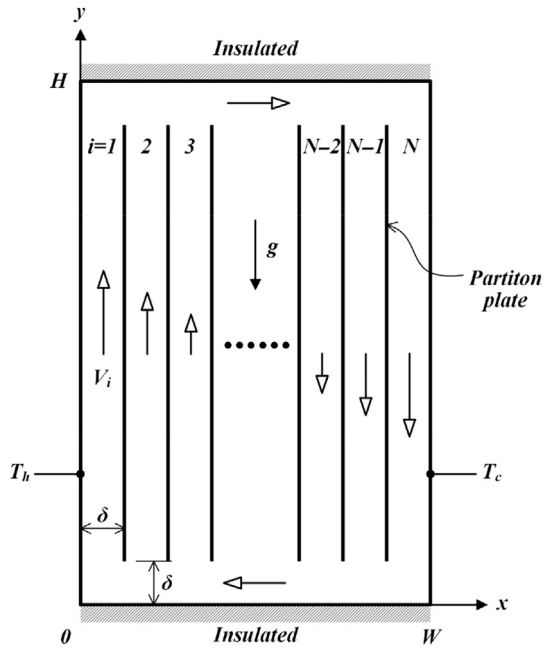

Fig. 1 – Schematic layout of a rectangular enclosure with multiple disconnected vertical partitions. δ, channel width; g, gravitational acceleration; H, enclosure height; i, layer index; N, number of fluid layers; T_c, cold wall temperature; T_h, hot wall temperature; V, mean velocity; W, enclosure width.

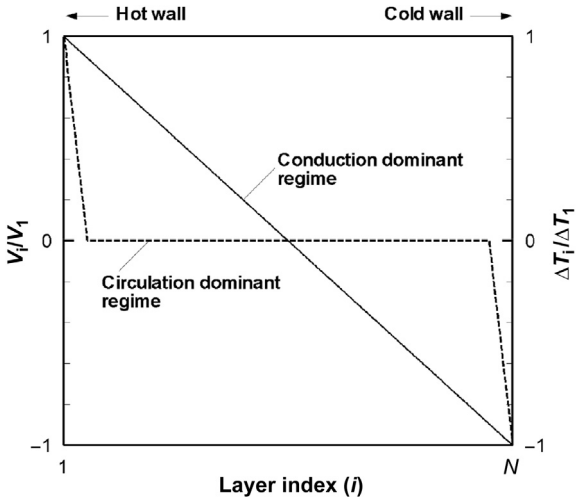

Fig. 2 – Illustration of velocity and temperature difference distributions in two limiting cases. ΔT, temperature difference; N, number of fluid layers; V, mean velocity.

In the present study, we investigated natural convection in a tall rectangular enclosure subjected to isothermal side boundary conditions with disconnected multiple vertical partitions of zero thickness. Under a fully developed laminar flow assumption, analytical modeling was performed to evaluate the flow rate of natural circulation and the average Nusselt number in a partially partitioned enclosure as a function of the main governing parameters such as the Rayleigh number, enclosure height/width ratio, and number of fluid layers. The validity and applicability of the proposed formulas are then established through comparisons with the numerical results. The impacts of the governing parameters on the emergence of natural circulation are also scrutinized along with a discussion of the heat transfer regimes.

2. Materials and methods

Fig. 1 shows a schematic diagram of the rectangular enclosure considered here, which is subjected to a horizontal temperature difference imposed over two isothermal side walls, with equally spaced vertical interior partitions separated from insulated top and bottom walls by a distance δ. To simplify the analysis, the following basic assumptions are made in this study, which are expected to be valid in many practical applications, such as multilayer insulation materials [11]: (1) the fluid channel width is small, such that $\delta \ll H$; (2) the vertical channel height is much larger than the enclosure width (i.e., $H \gg W$); (3) the interior partitions and exterior walls of the enclosure have no thickness; (4) the fluid properties are constant except for a linear density dependence on the temperature (Boussinesq approximation); (5) a steady, single-phase and fully developed laminar flow exists throughout the enclosure; (6) pressure losses in the miter bends and horizontal channels are negligibly small compared to

Table 1 – Nomenclature.

Nomenclature	
g	Gravitational acceleration
H	Enclosure height
$\dot{m}_{total}$	Circulation flow rate through the whole enclosure (per unit depth)
$\dot{m}_{outer}$	Circulation flow rate in the outermost loop (per unit depth)
N	Number of fluid layers
Nu_W	Average Nusselt number
Δp_b	Buoyancy head
Δp_f	Pressure loss
Pr	Prandtl number
Q_{cond}	Conductive heat transfer rate across the whole enclosure (per unit depth)
$Q_{NC,outer}$	Convective heat transfer rate in the outermost loop (per unit depth)
$Q_{NC,total}$	Convective heat transfer rate through the whole enclosure (per unit depth)
Ra_W	Rayleigh number
Ra^*	Modified Rayleigh number
Re_δ	Local Reynolds number
T_c	Cold wall temperature
T_h	Hot wall temperature
T_m	Mean temperature
ΔT	Temperature difference
V	Mean velocity
W	Enclosure width
Greek letters	
α	Thermal diffusivity
β	Thermal expansion coefficient
δ	Channel width
ζ_m	Ratio of circulation flow rate
ζ_q	Ratio of heat transfer rate
λ	Friction factor
ν	Kinematic viscosity
ρ	Density
Θ	Dimensionless bulk temperature
Ψ	Dimensionless heat transfer rate in the outermost loop
Superscript	
$+$	Nondimensionalization
Subscript	
i	Layer index

the wall friction in the vertical channels; and (7) thermal mixing in the horizontal channels (or gaps) is negligible.

Under these assumptions, the buoyancy-driven flow and heat transfer in a partially partitioned enclosure are expected to occur somewhere between the two limiting cases, namely, a conduction dominant regime and a circulation dominant regime. In the conduction dominant regime, the velocity magnitude of the buoyancy-driven flow in each vertical channel tends to vary linearly with layer index i, as illustrated in Fig. 2 (See Table 1 for a list of nomenclature used.). The mean velocity in each fluid layer relative to that in the first layer can be modeled by

$$\frac{V_i}{V_1} \approx \frac{2}{1-N}(i-1)+1, \tag{1}$$

where N is the number of vertical channels (or fluid layers) inside the enclosure and V_i is the mean velocity in each fluid layer. Then, the ratio of circulation flow rate between the whole enclosure and the outermost loop can be approximated as

$$\zeta_m = \frac{\dot{m}_{total}}{\dot{m}_{outer}} = \frac{1}{2}\sum_{i=1}^{N}\left|\frac{V_i}{V_1}\right| \approx \sum_{i=1}^{\frac{N+1}{2}}\left(\frac{2i}{1-N}+\frac{N+1}{N-1}\right) = \frac{N+1}{4} \tag{2}$$

By contrast, in the circulation dominant regime, the buoyancy-driven flow is expected to circulate only through the outermost loop with quiescent fluids at the inner loops, and the circulation flow rate ratio approaches unity.

Likewise, the ratio of the natural convection heat transfer rate through the whole enclosure to that in the outermost loop can be expressed as

$$\zeta_q = \frac{Q_{NC,total}}{Q_{NC,outer}} = \frac{1}{2}\sum_{i=1}^{N}\left|\frac{V_i\Delta T_i}{V_1\Delta T_1}\right| \approx \sum_{i=1}^{\frac{N+1}{2}}\left(\frac{2i}{1-N}+\frac{N+1}{N-1}\right)^2 \approx \begin{cases} \frac{N}{6} & : conduction\ regime \\ 1 & : circulation\ regime \end{cases} \tag{3}$$

In the above, it has been assumed that $\Delta T_i/\Delta T_1$ and V_i/V_1 have the same curves, where ΔT_i indicates the temperature difference that arises from natural circulation between the inlet and outlet of each fluid layer, i.e., in the conduction dominant regime, the temperature difference decreases linearly toward the center of the enclosure, whereas it remains zero except for the outermost loop in the circulation dominant regime as depicted in Fig. 2.

The average Nusselt number, defined as the ratio of overall heat transfer rate to the pure conduction across the whole enclosure, is given by

$$Nu_W = \frac{Q_{cond}+Q_{NC,total}}{Q_{cond}} = 1+\zeta_q\Psi, \tag{4}$$

where the dimensionless heat transfer rate arising from the natural circulation in the outermost loop is

$$\Psi = \frac{Q_{NC,outer}}{Q_{cond}} = \frac{\dot{m}_{outer}c_p(T_h-T_c)}{\frac{kH}{W}(T_h-T_c)} = Re_{\delta,1}Pr\frac{W}{H} \tag{5}$$

Here, $Re_\delta = V\delta/\nu$ is the local Reynolds number based on the channel width and $Pr = \nu/\alpha$ is the Prandtl number. In Eq. (4), it is important to note that if Ψ is sufficiently small (e.g., $\Psi \ll 1$), the heat transfer in the partially partitioned enclosure will be mainly attributed to the conduction. By contrast, when Ψ is large enough (e.g., $\Psi \gg 1$), the natural convection dominates over the conductive heat transfer. This suggests that Ψ may be used to characterize the heat transfer regime. Hence, for the general case, the ratio of the circulation flow rate through the whole enclosure to the one in the outermost loop, can be computed by the linear interpolation between the two extreme values of ζ_m using a weighting factor of $1/(1+\Psi)$ as follows

$$\zeta_m = \frac{1}{1+\Psi}\frac{N+1}{4}+\frac{\Psi}{1+\Psi} \tag{6}$$

Similarly, the ratio of heat transfer rates in the whole enclosure and the outer loop is proposed as

$$\zeta_q = \frac{1}{1+\Psi}\frac{N}{6}+\frac{\Psi}{1+\Psi} \tag{7}$$

The average Nusselt number is then rewritten by

$$Nu_W = 1 + \frac{\Psi}{1+\Psi}\frac{N}{6} + \frac{\Psi^2}{1+\Psi} \quad (8)$$

In Eqs. (6–8), it is worth noting that once $\Psi \to 0$ (i.e., conduction dominant regime), then $\zeta_m \to (N+1)/4$ and $\zeta_q \to N/6$, and $Nu_W \to 1$. By contrast, if $\Psi \to \infty$ (i.e., circulation dominant regime), then $\zeta_m \to 1$ and $\zeta_q \to 1$, and $Nu_W \to \Psi$.

In order to derive the expression for Ψ, attention is next paid to the buoyancy-driven flow circulating through a single closed loop that involves two parallel vertical channels with heating and cooling, respectively (i.e., first layer and Nth layer in Fig. 1). Under the assumptions described above, the momentum equation reads as

$$\Delta p_b = \Delta p_f \quad (9)$$

in which the buoyancy head integrated over the loop is given by

$$\Delta p_b = \rho\beta(T_h - T_c)gH(1-2\Theta), \quad (10)$$

where ρ is the fluid density, β is the thermal expansion coefficient, and g is the gravitational acceleration. In Eq. (10), Θ refers to the dimensionless bulk temperature in the channel and is defined as

$$\Theta = \frac{1}{H^+}\int_0^{H^+}\frac{T_m - T_c}{T_h - T_c}dy^+ \quad (11)$$

where T_m is the mean temperature weighted with respect to the vertical velocity, and the superscript $+$ represents the nondimensionalization using $\delta Re_\delta Pr$. When the channel height is larger than the thermal development length, Θ can be approximated by

$$\Theta \approx 0.3733\frac{\delta Re_{\delta,1}Pr}{H}, \quad (12)$$

which is obtained from the analytic solution to the parallel-plate channel with one side of constant temperature [12].

Presuming that frictional losses in the vertical channels dominate over all form losses, the pressure drop in Eq. (9) can be expressed by

$$\Delta p_f = \rho\lambda\left(\frac{H}{2\delta}\right)V_1^2, \quad (13)$$

where λ is the friction factor. For the two-dimensional laminar flow (i.e., $\lambda = 48/Re_\delta$) considered here [13], the above equation is rewritten as

$$\Delta p_f = \frac{24\mu^2}{\rho\delta^2}\left(\frac{H}{\delta}\right)Re_{\delta,1} \quad (14)$$

Combining Eqs. (9), (10), (12), and (14) yields the local Reynolds number in the first layer (or Nth layer)

$$Re_{\delta,1} = \frac{\beta(T_h - T_c)g\delta^3\nu^{-2}}{0.7466\beta(T_h - T_c)g\delta^3\nu^{-2}\left(\frac{\delta}{H}\right)Pr + 24}, \quad (15)$$

where ν is the kinematic viscosity. Then, by substituting Eq. (15) into Eq. (5) and using $\delta = W/N$, one obtains

$$\Psi = \frac{N}{0.7466 + 24N^4\left(\frac{H}{W}\right)Ra_W^{-1}} \quad (16)$$

in which the Rayleigh number is defined by

$$Ra_W = \frac{\beta(T_h - T_c)gW^3}{\alpha\nu} \quad (17)$$

Here, the fluid properties α, β, and ν are evaluated at the reference temperature $T_f = (T_h + T_c)/2$, where T_h and T_c are the hot and cold wall temperatures, respectively. From Eq. (16), it can be conjectured that Ψ increases with an increase in the Rayleigh number Ra_W (or temperature difference between the exterior side walls), whereas it decreases with an increase in the enclosure height/width ratio (H/W) or the number of fluid layers N.

3. Results

In order to assess the validity of the proposed expressions for the circulation flow rate and average Nusselt number in a tall rectangular enclosure with disconnected vertical partitions inside (Fig. 1), a series of two-dimensional numerical simulations are performed using a commercial computational fluid dynamics code, Fluent 12.0 [14], for channel width/height ratios of 4×10^{-4}–1.4×10^{-3}, number of fluid layers of 4–20, and Rayleigh numbers of up to 3.4×10^7. Pressure–velocity coupling is achieved via the SIMPLE algorithm [15], and a second-order upwind method is used for the discretization of momentum and energy equations. As for the boundary conditions of the enclosure, no-slip adiabatic wall conditions are set on the top and bottom boundaries, whereas no-slip isothermal boundary conditions of different temperatures are applied at the side walls. The simulations are conducted on the grid system composed of $40\times2{,}280$ cells in each fluid layer, with a minimum grid spacing of 0.01δ, which is chosen based on additional grid dependency tests. The maximum residual tolerance was set to 10^{-10} in all simulations as the convergence criteria, and we have confirmed that a steady state is always reached.

Fig. 3 shows isotherms in the partially partitioned enclosure for $N = 20$ at various modified Rayleigh numbers, $Ra^* = (W/H)Ra_W$. At $Ra^* = 6.3\times10^3$, isotherms are arranged parallel to the side walls of the enclosure and are uniformly spaced in the horizontal direction, except for the region near the top and bottom walls, implying that the temperature varies almost linearly with distance along the x axis and the conduction dominates the overall heat transfer. When Ra^* increases, the isotherms tend to flatten (perpendicular to the side walls) in the central part of the enclosure, whereas closely spaced isotherms representing a steep temperature gradient are presented near the side walls. These results indicate that the temperature variation within the fluid layer diminishes inward from the sides into the center of the enclosure, and the heat transfer regime changes from conduction to a circulation dominant regime with increases in the modified Rayleigh number.

The impact of the modified Rayleigh number on the formation of natural circulation inside the enclosure is then shown in Fig. 4, where the mean velocity of the buoyancy-driven flow in each fluid layer relative to that in the first layer

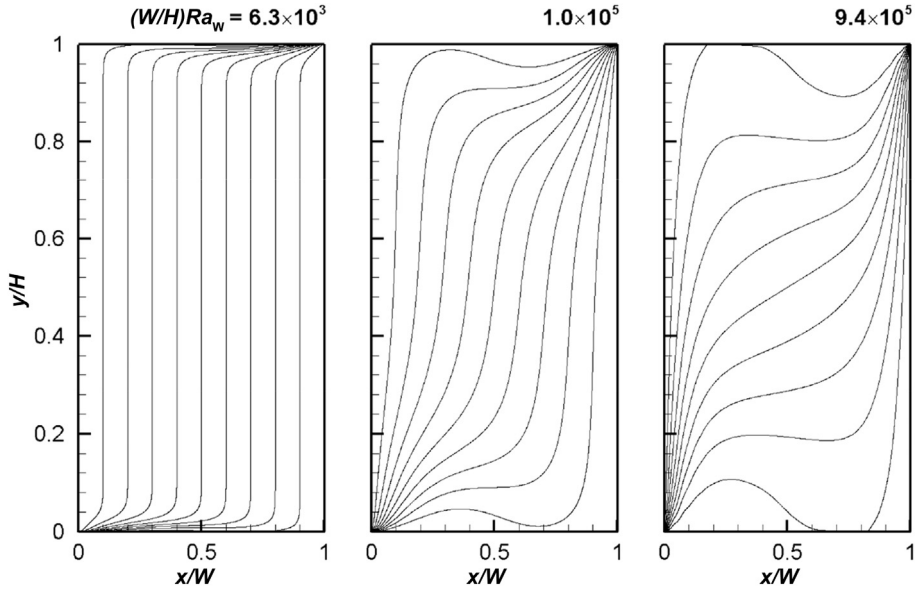

Fig. 3 – Isotherms for N = 20 at various modified Rayleigh numbers $Ra^* = (W/H)Ra_W$. H, enclosure height; W, enclosure width.

is plotted for $N = 20$. At $Ra^* = 6.3 \times 10^3$ (i.e., conduction dominant regime), it is observed that similar to the temperature distribution, the mean velocity variation is almost linear with the layer index. By contrast, at a higher Ra^*, the velocity magnitude is found to decrease nonlinearly toward the center of the enclosure, and its reduction rate increases with increases in Ra^*. Together with the numerical results depicted in Fig. 3, this observation provides justification for the assumptions used to evaluate ζ_m and ζ_q of Eqs. (2) and (3), and suggests again that the effect of natural convection becomes increasingly significant with increases in the modified Rayleigh number.

Fig. 5 displays the variation of the local Reynolds number in the first layer with the channel width/height ratio (δ/H) and the number of fluid layers, N. The overall agreement between the results obtained from numerical simulations and the prediction of Eq. (15) is shown to be favorable, although the analytical model slightly overestimates the local Reynolds number in the first layer because the pressure losses in the miter bends and gaps are neglected in Eq. (15). It is also noteworthy that a rise in the channel width/height ratio results in an increase in $Re_{\delta,1}$, which appears to be less dependent on the number of fluid layers. This is expected to be mainly because of the decreasing wall friction in the fluid layer at a greater δ/H.

Fig. 6 compares the normalized circulation flow rate through the whole enclosure between the numerical results

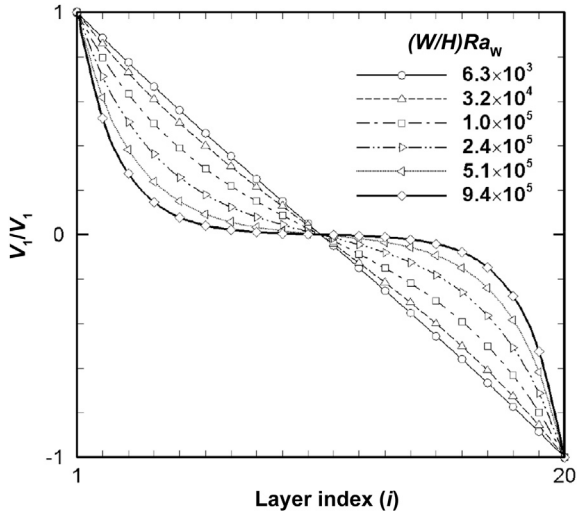

Fig. 4 – Mean velocity distribution for N = 20 at various modified Rayleigh numbers: numerical results. $(W/H)Ra_W$, modified Rayleigh number; V, mean velocity.

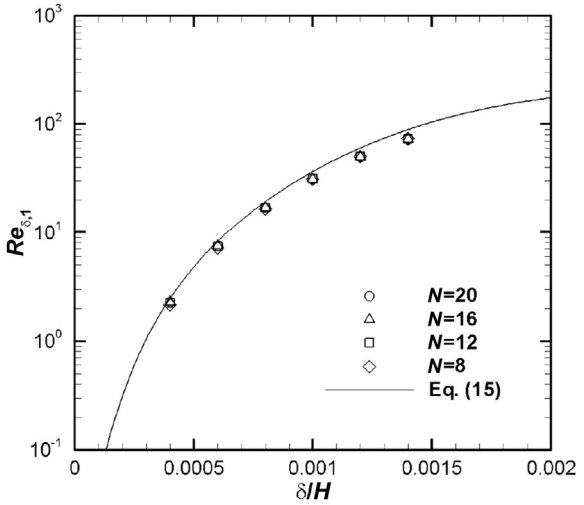

Fig. 5 – Influence of channel width to height ratio on local Reynolds number in the first layer. Symbols represent the numerical results and the solid line is the prediction of Eq. (15). δ, channel width; H, enclosure height; N, number of fluid layers; Re_δ, local Reynolds number.

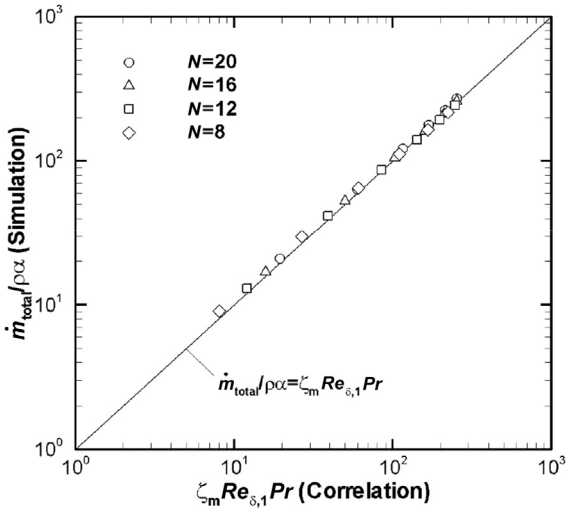

Fig. 6 – Comparison of total circulation flow rate (normalized by ρα) between the numerical results (symbols) and the prediction using Eqs. (6) and (15). α, thermal diffusivity; $\dot{m}_{total}$, circulation flow rate through the whole enclosure (per unit depth); N, number of fluid layers; Pr, Prandtl number; Re_δ, local Reynolds number; ρ, density; ζ_m, ratio of circulation flow rate.

and the prediction based on Eqs. (6) and (15). It can be seen that in all the cases tested, numerical data are correlated satisfactorily and are fitted quite well by the proposed description of ζ_m and $Re_{\delta,1}$. Fig. 7 shows the relationship between the average Nusselt number and modified Rayleigh number for various numbers of fluid layers. As expected, the Nusselt number is found to increase with an increase in the modified Rayleigh number, i.e., convective heat transfer arising from natural circulation is more pronounced as Ra^* increases. One can also see that for a given Ra^*, the Nusselt number decreases with an increase in the number of fluid layers (or insertion of partitions), the effect of which becomes prominent at a higher Ra^*. Moreover, it is interesting to note that Eqs. (8) and (16) provide a fairly good approximation of the Nusselt number with a maximum relative error of less than 10% in the range of $4 \leq N \leq 20$ and $Ra^* \leq 10^6$. This supports the validity of the present analytical model for laminar natural convection in a partially partitioned enclosure.

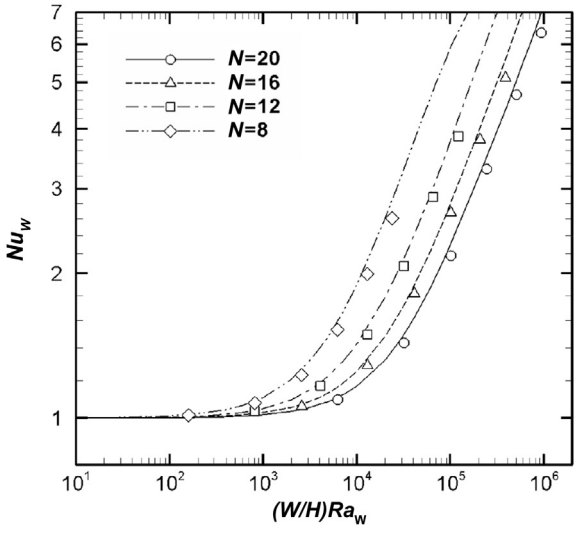

Fig. 7 – Average Nusselt number versus modified Rayleigh number relationship for various N values. Symbols represent the numerical results and the lines are drawn using Eqs. (8) and (16). N, number of fluid layers; Nu_w, average Nusselt number; $(W/H)Ra_w$, modified Rayleigh number.

4. Conclusion

In the present study, we investigated the laminar natural convection in a tall rectangular enclosure with isothermal side walls of different temperatures and insulated top and bottom walls with disconnected multiple vertical partitions inside. Based on the analytical modeling work, the formulas were suggested to predict the circulation flow rate and average Nusselt number, being expressed as a function of Rayleigh number, enclosure height/width ratio, and the number of fluid layers. The formulas are then validated through comparisons with results obtained from numerical simulations for modified Rayleigh numbers of up to 10^6. It is shown that the average Nusselt number increases with increases in the modified Rayleigh number, but decreases with increases in the number of fluid layers. The obtained results also indicate that within the limitations of constant fluid properties with Boussinesq approximation and isothermal side walls, the proposed formulas can provide a simple way to estimate the heat transfer augmentation caused by the gaps in a tall partitioned enclosure, with their applications to design and manufacture of multilayer insulation materials.

Conflict of interest

The authors declare that they have no conflict of interest.

Acknowledgements

This work was supported by the National Research Foundation of Korea (NRF) funded by the Korea government (MSIP) (No. NRF-2012M2A8A4025974).

REFERENCES

[1] R. Anderson, A. Bejan, Heat transfer through single and double vertical walls in natural convection: theory and experiment, Int. J. Heat Mass Transfer 24 (1981) 1611–1620.
[2] T. Nishimura, M. Shiraishi, F. Nagasawa, Y. Kawamura, Natural convection heat transfer in enclosures with multiple vertical partitions, Int. J. Heat Mass Transfer 31 (1988) 1679–1686.
[3] H. Turkoglu, N. Yücel, Natural convection heat transfer in enclosures with conducting multiple partitions and side walls, Heat Mass Transfer 32 (1996) 1–8.

[4] V. Sambou, B. Lartigue, F. Monchoux, J.L. Breton, One-dimensional model of natural convection in differentially heated partitioned enclosures with conducting external walls and vertical partitions, J. Thermal Sci. Eng. Appl. 1 (2009) 021002.
[5] T.W. Tong, F.M. Gerner, Natural convection in partitioned air-filled rectangular enclosures, Int. Commun. Heat Mass Transfer 13 (1986) 99–108.
[6] C.J. Ho, Y.L. Yih, Conjugate natural convection heat transfer in an air-filled rectangular cavity, Int. Commun. Heat Mass Transfer 14 (1987) 91–100.
[7] A. Kangni, R. Ben Yedder, E. Bilgen, Natural convection and conduction in enclosures with multiple vertical partitions, Int. J. Heat Mass Transfer 34 (1991) 2819–2825.
[8] E. Bilgen, Natural convection in enclosures with partial partitions, Renewable Energy 26 (2002) 257–270.
[9] V. Costa, M. Oliveira, A. Sousa, Mixed laminar free convective flows in enclosures with arrays of partial partitions — a numerical study, Proceedings of HT2003, ASME Summer Heat Transfer Conference, Nevada, USA, 2003.
[10] S.H. Kim, Y.I. Kim, C.T. Park, S. Choi, J. Yoon, Effect of gaps on the performance of the vertically installed wet thermal insulator, Proceedings of the 2012 International Congress on Advances in Nuclear Power Plants (ICAPP '12), Chicago, USA, 2012.
[11] M.M. Finckenor, D. Dooling, Multilayer Insulation Material Guidelines, NASA/TP-1999–209263, 1999.
[12] Y. Bae, S.H. Kim, J.K. Seo, Y.I. Kim, Numerical analysis of thermal development of laminar flow in a concentric multilayer annulus, Chem. Eng. Technol. 37 (2014) 123–130.
[13] R.D. Blevins, Applied Fluid Dynamics Handbook, Van Nostrand-Reinhold, New York, 1984.
[14] ANSYS Inc, Fluent 12.0 Theory Guide, 2009.
[15] S.V. Patankar, Numerical Heat Transfer and Fluid Flow, Hemisphere Publishing Corp., New York, 1980.